Stress Singularities in a Model of a Wood Disk under Sinusoidal Pressure

Jay A. Johnson[1]; John C. Hermanson[2]; Steven M. Cramer, M.ASCE[3]; and Charles Amundson[4]

Abstract: A thin, solid, circular wood disk, cut from the transverse plane of a tree stem, can be modeled as a cylindrically orthotropic elastic material. It is known that a stress singularity can occur at the center of a cylindrically orthotropic disk subjected to uniform pressure. If a solid cylindrically orthotropic disk is subjected to sinusoidal pressure distributions, then other stress singularities can also occur in the disk. The criterion for the existence of these singularities is based on a simple relationship between two dimensionless elastic constant parameters and the sinusoidal pressure loading mode number. For a given set of elastic constants, only a finite number of lower sinusoidal modes will produce stress singularities. In this paper, the mathematical relationships between these parameters are derived.

DOI: 10.1061/(ASCE)0733-9399(2005)131:2(153)

CE Database subject headings: Anisotropic materials; Elastic analysis; Mathematical models; Stress analysis; Wood products; Pressures.

Introduction

The stem of a tree has the shape of a tapered cylinder whose cross section is approximately circular. Due to variations in wood cell characteristics that occur during the growing season, circular (or almost circular) wood density patterns can be seen in the cross section. These patterns, tree rings, are familiar to almost everyone. The tree rings, and other anatomical features of wood, suggest that the cylindrical coordinate system (r,θ,z) would be a good candidate for modeling the material organization of thin disks of this biological material (Fig. 1).

It follows that three mutually perpendicular unit vectors can be associated with each point in the wood disk: $\hat{\mathbf{e}}_R$, in the radial direction (R or r), $\hat{\mathbf{e}}_T$, in the tangential direction (T or θ), and $\hat{\mathbf{e}}_L$, in the longitudinal direction (L or z). Some physical and mechanical properties of wood take on values that are different in these anatomical directions. In particular, Young's moduli are roughly in the ratios of $E_L:E_R:E_T=20:2:1$. It should be noted, however, that the determination of the elastic constants generally involve the use of rectilinearly shaped test specimens in which rectilinear orthotropy has been assumed; see Kollman and Côté (1964, p. 304, Fig. 7.10) for a graphic example. For the transverse plane of wood, a more appropriate assumption would be to invoke cylindrical orthotropy (CYO) that mimics the anatomical material organization.

The motivation for the work presented here stems from the desire to obtain accurate values for the transverse constants of wood that preserve the anatomical arrangement to calculate the transverse properties. These transverse properties will be useful for simulations of drying stresses, in structural analysis such as small-diameter timber structures and other structural applications that require the complete set of three dimensional elastic constants. A test protocol is being sought that applies radial and tangential point loads and measures radial and tangential displacements to determine the values of the elastic constants. By developing theoretical expressions for the displacements of CYO test specimens subjected to known point loading patterns, an inverse method can be used to determine the elastic parameters from the measured boundary conditions. Since point loads can be represented by generalized functions—delta functions in the form of Fourier series—it was natural to express the stress function in the form of a Fourier series with coefficients being functions of the radial coordinate only. While searching for appropriate theoretical expressions to be used in the test protocol, stress singularities were noticed in solid CYO disks that were subjected to certain sinusoidal pressure distributions on the outer circumferential surfaces. The purpose of this paper is to elaborate the conditions that lead to these stress singularities.

Generalized Hooke's law for a CYO elastic material can be expressed in a dimensionless form as

$$\begin{Bmatrix} \epsilon_r \\ \gamma_{r\theta} \\ \epsilon_\theta \end{Bmatrix} = \begin{bmatrix} a & 0 & -\nu\sqrt{a} \\ 0 & 2(b+\nu\sqrt{a}) & 0 \\ -\nu\sqrt{a} & 0 & 1 \end{bmatrix} \begin{Bmatrix} \sigma_r/E_T \\ \tau_{r\theta}/E_T \\ \sigma_\theta/E_T \end{Bmatrix} \tag{1}$$

The notation for the cylindrical stress and strain components are those used by Timoshenko and Goodier (1970), i.e., σ is used for normal stress, τ is used for shear stress, ε is used for normal strain, and γ is used for shear strain. Generalized Hooke's law expressed in this form reveals that the essential relationship be-

[1]Professor, Dept. of Wood and Paper Science, Univ. of Washington, Mail Stop 352100, Seattle, WA 98195.

[2]Research General Engineer, USDA Forest Service Forest Products Laboratory, One Gifford Pinchot Dr., Madison, WI 53726-2398. E-mail: jhermanson@fs.fed.us

[3]Professor, Dept. of Civil and Environmental Engineering, Univ. of Wisconsin–Madison, 2266 Engineering Hall, 1415 Engineering Dr., Madison, WI 53706.

[4]Graduate Student, Univ. of Washington, Mail Stop 352100, Seattle, WA 98195.

Note. Associate Editor: Ronald Y. S. Pak. Discussion open until July 1, 2005. Separate discussions must be submitted for individual papers. To extend the closing date by one month, a written request must be filed with the ASCE Managing Editor. The manuscript for this paper was submitted for review and possible publication on August 23, 2002; approved on May 13,2004. This paper is part of the *Journal of Engineering Mechanics*, Vol, 131, No. 2, February I, 2005. ©ASCE, ISSN 0733-9399/2005/2-153–160/$25.00.

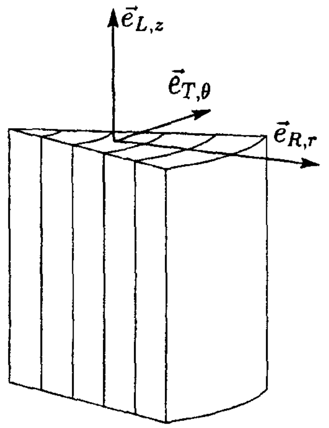

Fig. 1. Wood modeled by principal material directions of cylindrical coordinate system

tween the stress and strain components is determined by three dimensionless parameters– *a, b,* and ν –and a scaling parameter E_T. The dimensionless elastic parameters are related to the traditional elastic constants by

$$\nu = \sqrt{\nu_{RT}\nu_{TR}}$$

$$a = \frac{E_T}{E_R} \tag{2}$$

$$b = \frac{1}{2}\left(\frac{E_T}{G_{RT}}\right) - \nu\sqrt{a}$$

where E=Young's moduli; G=shear moduli; and ν=Poisson's ratios. Values of the elastic constants for several species of North American woods can be found in several sources: Hearmon (1961); Kollman and Côté (1964); Bodig and Goodman (1973); Bodig and Jayne (1982); Forest Products Laboratory (1999); to name a few. The symbols used above for the elastic constants and for the subscripts for the principal material directions– *R, T, L* –are commonly used in the wood science literature.

A solution technique for determining the stress components in a CYO material has been developed (Lekhnitskii 1963, Chap. 4). The technique involves a stress function ϕ which, once determined, can be used to compute the stress components, σ_r, σ_θ, and $\tau_{r\theta}$. Others have used a CYO material formulation to model the elastic behavior of wood or paper. Drying stresses in wood have been investigated using the CYO material assumption (Johnson 1975). Stress development in the winding of paper rolls has been examined (Roisum 1994). A theory of growth stress in trees has been developed (Archer 1987). Approximate stress distribution in wood disks has been modeled by Hermanson (1992) using a novel finite element formulation that incorporates the concept of curvilinear elasticity.

It is well known from the work of Lekhnitskii (1963) that a solid CYO disk subjected to a uniform pressure on the outer circumferential surface will exhibit both radial and tangential stress singularities if $a < 1$. Lekhnitskii uses n^2 for a. During the past decades, several papers have been published which have revealed stress singularities due to the mechanical response of nonisotropic materials in various configurations subjected to certain types of loads. Antmann and Negron-Marréro (1987) have uncovered stress singularities in various types of nonlinear aeolotropic materials subjected to radially symmetric loading. Ting (1999c) has further amplified this work and has detailed the nature of the stress singularities found in spherically anisotropic solids under uniform radial pressure. Horgan and Baxter (1996) have studied the stress distributions in hollow disks under axisymmetric loading and have noted the locations of maximum stress when the outer-to-inner radii of the disk increases without bound. Using a thick disk, in fact a cylinder, of CYO material with a wedge removed, Ting (1997) showed that there is a stress singularity at the wedge apex when the wedge surfaces are subjected to equal but oppositely directed uniform shear distributions. Ting (1999a,b) has elaborated on this phenomenon and showed that for any wedge angle there exists a combination of elastic properties that will cause the stress singularity to disappear. The problem of stress singularities associated with sharp notches or cracks will not be addressed in this paper. We will discuss a new type of stress singularity, one associated with the cylindrical organization of material stress, and the interaction of this material with sinusoidal pressurized loading.

In the following sections, stress distributions will be obtained for specific applied sinusoidal pressure modes, labeled by the index n. The purpose of the analysis will be to show that under certain conditions external sinusoidal loading will give rise to stress singularities. The conditions giving rise to the stress singularities will be displayed graphically in a two-dimensional plot of the dimensionless elastic parameters *a* and *b*.

Mathematical Model

To display the conditions necessary for the existence of stress singularities in CYO solid disks under sinusoidal loading, a general solution to the stress function will be found. Then a particular solution for each term of a self-equilibrated pressure distribution applied to the outer surface of the disk will be determined. No tangential shearing distributions will be allowed on the outer surface. Clearly, a wide range of solutions for the stresses, strains, and displacements in the solid disks can be obtained from these solutions by superimposing the results associated with each term. However, only three cases will be considered in this paper: the uniform load case ($n=0$), a special case ($n=1$), and the general case ($n=2,3,...$). It should be noted that the special case (n $=1$) is not a self-equilibrating pressure distribution applied to a disk. A shear distribution must be present to have force equilibrium. It is included in the following discussion only to show that this unique case will not yield stress singularities.

For plane stress problems involving thin disks, a Fourier series in which the Fourier coefficients ϕ_k and $\bar{\phi}_k$ are functions of the radial coordinate can be assumed as a general form for a stress functionsolution

$$\phi(r,\theta) = \phi_0(r) + \sum_{k=2}^{\infty}\{\phi_k(r)\cos(k\theta) + \bar{\phi}_k(r)\sin(k\theta)\} \tag{3}$$

Given a self-equilibrated pressure distribution (Fig. 2) acting at the outer surface of a solid disk $r=r_0$

$$p(\theta) = p_0 + \sum_{k=2}^{\infty} p_k\cos(k\theta) \tag{4}$$

it can be shown that each of the coefficients ϕ_k of the stress function will be functions of r and the known parameters k, p_k, a, b, and r_0. The stress components in the disk will be the sum total of the stresses corresponding to each term in the expression for the external pressure. Each term in this pressure distribution, except for p_0, represents a sinusoidal pressure that exhibits k compression, or tension, cycles around the circumference. The index k can be thought of as a sinusoidal pressure distribution mode number.

The mathematical procedure for determining stresses in a CYO material is well documented (Lekhnitskii 1963). A summary of the essential steps follows. Summarizing these steps may appear to be repetitious and unnecessary, given Lekhnitskii's work, but the development used in this paper differs slightly in notation and presentation. Our notation effectively illuminates how the state of stress in wood disks, modeled as a CYO material, is related to essential nondimensional elastic parameters: a, b, and ν. Three differential operators (D_1, D_2, and D_3) are used to define the stress from the stress function ϕ

$$\sigma_r = \mathcal{D}_1(\phi)$$

$$\tau_{r\theta} = \mathcal{D}_2(\phi) \tag{5}$$

$$\sigma_\theta = \mathcal{D}_3(\phi)$$

where

$$\mathcal{D}_1 \equiv \frac{1}{r}\left\{\frac{\partial}{\partial r} + \frac{1}{r}\frac{\partial^2}{\partial\theta^2}\right\}$$

$$\mathcal{D}_2 \equiv -\frac{1}{r}\frac{\partial}{\partial\theta}\left\{\frac{\partial}{\partial r} - \frac{1}{r}\right\}$$

$$\mathcal{D}_3 \equiv \frac{\partial^2}{\partial r^2}$$

This definition assures force equilibrium for any infinitesimal volume element within the CYO disk. Another three differential operators place a constraint on the strain components to maintain displacement continuity

$$\mathcal{D}_4(\epsilon_r) + \mathcal{D}_5(\gamma_{r\theta}) + \mathcal{D}_6(\epsilon_\theta) = 0 \tag{6}$$

where these three operators are similar to, but not the same as, the first three

$$\mathcal{D}_4 \equiv -\frac{1}{r}\left\{\frac{\partial}{\partial r} - \frac{1}{r}\frac{\partial^2}{\partial\theta^2}\right\}$$

$$\mathcal{D}_5 \equiv -\frac{1}{r}\frac{\partial}{\partial\theta}\left\{\frac{\partial}{\partial r} + \frac{1}{r}\right\}$$

$$\mathcal{D}_6 \equiv \frac{\partial^2}{\partial r^2} + \frac{2}{r}\frac{\partial}{\partial r}$$

By combining the displacement compatibility relationship Eq. (6) with generalized Hooke's law Eq. (1) and utilizing the stress function definition Eq. (5), a fourth order partial differential equation for the stress function is obtained that consists of two parts

$$\mathcal{L}(\phi) = \mathcal{L}_1(\phi) - \nu\sqrt{a}\mathcal{L}_2(\phi) = 0 \tag{7}$$

where

$$\mathcal{L}_1 \equiv \mathcal{D}_6\mathcal{D}_3 + 2b\mathcal{D}_5\mathcal{D}_2 + a\mathcal{D}_4\mathcal{D}_1$$

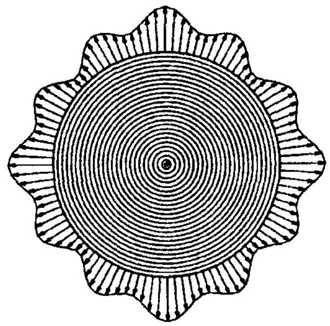

$$p(\theta) = p_o + \sum_{k=2}^{\infty} p_k \cos(k\theta)$$

Fig. 2. Self-equilibrated pressure distribution represented as cosine Fourier series

$$\mathcal{L}_2 \equiv \mathcal{D}_6\mathcal{D}_1 - 2\mathcal{D}_5\mathcal{D}_2 + \mathcal{D}_4\mathcal{D}_3$$

When a stress function in the form of Eq. (3) is acted upon by the operator of Eq. (7), another Fourier series expression will be obtained. It is easily verified that the second operator in Eq. (7) will annihilate the stress function, so its solution will not contain the parameter ν. Since the resulting expression must be equal to zero at every point in the disk, the coefficients of the $\cos(k\theta)$ and $\sin(k\theta)$ terms must be equal to zero. It follows that a sequence of fourth order, ordinary differential equations will be obtained for these coefficients and they will have the form

$$r^4y'''' + Ar^3y''' + Br^2y'' + Cry' + Dy = 0 \tag{8}$$

where y represents each of the coefficients ϕ_k and A, B, C, and D = constants involving a and b and the loading mode parameter k. The form of Eq. (8) is a generalized form of the Euler equation, found in elementary differential equation textbooks, and is easily transformed to a new differential equation with constant coefficients by $x = \ln(r)$. The general solution is

$$y = K_1e^{\mu_1 x} + K_2e^{\mu_2 x} + K_3e^{\mu_3 x} + K_4e^{\mu_4 x} \tag{9}$$

where K_j = constants of integration to be determined by the boundary conditions and μ_j ($j = 1,2,3,4$) = four roots of the characteristic polynomial

$$P_k(\mu,a,b) = (\mu-1)^4 - (1 + a + 2bk^2)(\mu-1)^2 + (k^2-1)^2a \tag{10}$$

associated with the differential equations of Eq. (8). Selecting a and b as symbols for the dimensionless elastic parameters leads to elementary and elegant expressions for the roots of the characteristic polynomial Eq. (10) which turns out to be a simple quadratic expression in $(\mu-1)^2$. Replacing x by $\ln(r)$, y by ϕ_k in Eq. (9), and summing the terms, a general solution for the stress function is found

$$\phi(r,\theta) = \sum_{j=1}^{4} K_{0j}r^{\mu_{0j}} + \sum_{k=1}^{\infty}\left\{\sum_{j=1}^{4}\left[K_{kj}r^{\mu_{kj}}\cos(k\theta) + \bar{K}_{kj}r^{\mu_{kj}}\sin(k\theta)\right]\right\} \tag{11}$$

in which the roots $\mu_{k1} < \mu_{k2} < \mu_{k3} < \mu_{k4}$ are given by the formulas

$$\mu_{01}=0$$

$$\mu_{02}=1-\sqrt{a}$$

$$\mu_{03}=1+\sqrt{a}$$

$$\mu_{04}=2$$

$$\mu_{k1}=1-k\chi_{k1} \qquad (12)$$

$$\mu_{k2}=1-k\chi_{k2}$$

$$\mu_{k3}=1+k\chi_{k2}$$

$$\mu_{k4}=1+k\chi_{k1}$$

with

$$\chi_{k1,2}^2=\left(b+\frac{(1+a)}{2k^2}\right) \pm\sqrt{\left(b+\sqrt{a}+\frac{(1-\sqrt{a})^2}{2k^2}\right)\left(b-\sqrt{a}+\frac{(1+\sqrt{a})^2}{2k^2}\right)}$$

The parameters χ_{k1} and χ_{k2}, exponents of the radial coordinate as determined by the expression in Eq. (12), are similar, if not the same as, the exponents found by Ting [1999b, p. 391, Eq. (3.9)]. Ting's exponents, however, are not restricted to integral modes and were obtained by other means. To specifically determine the stresses in a thin wood disk of thickness h and outer radius r_0 ($h \ll r_0$) subject to an external sinusoidal pressure distribution, $p = p_n\cos(n\theta)$ ($n>1$), it is necessary to apply appropriate boundary conditions. Since this pressure distribution has no $\sin(k\theta)$ terms, all the $\bar{K}_{kj}$ of Eq. (11) will be zero. Moreover, only the coefficients associated with $k=n$ [the $\cos(n\theta)$ term] will not be zero, i.e., $K_{kj}=0$ except for $k=n$. The displacements at the center of the disk must be zero, which implies that K_{n1} and K_{n2} will be equal to zero. Finally, K_{n3} and K_{n4} can be found from the fact that at $\sigma_r = p_n\cos(n\theta)$ and $\tau_{r\theta}=0$ at $r=r_0$. With the stress function completely specified by known values of the K_{nj} and the μ_{nj}, the state of stress in the solid disk can be determined utilizing the first three differential operators of Eq. (5).

Finite Element Approximations

The nature of the stress singularities due to sinusoidal loading will be presented in the next section. Since the analytic results reveal large changes over small regions near the center of the CYO disk, it would appear that numerical methods might run into difficulties relative to approximating these rapidly changing stress variations. We performed a standard, unsophisticated finite element (FE) analysis to assess the degree to which these difficulties might manifest themselves. Most commercially available FE codes contain provisions for rectilinearly orthotropic (REO) materials. Generally, it is possible to specify` an orientation parameter, such as the angle between one of the principal material directions and one of the global coordinate directions for each element in the mesh, and the FE code will transform the material stiffness tensor appropriately. This approximation technique will account for the local stiffness orientation of the material. Obviously, if the element is small the deviation between the CYO orientation pattern and the approximate REO orientation at each point in the element will be small. Near the center of the disk, however, the material direction changes very sharply and the material characterization may not be accurate. Replacing the cylindrically orthotropic orientation pattern of a *CYO* material with a homogeneous orientation of a REO material within the domain of an element will be called a patchwise rectilinear orthotropic (PRO) approximation analysis.

A disk of wood was modeled as a quarter circle with two planes of symmetry, i.e., $\theta=0$ and $\theta=\pi/2$. An FE mesh, consisting of 1,411 nodes, 435 quadrilateral, isoparametric elements (8 nodes), and 15 triangular isoparametric elements (6 nodes) at the center of the disk, was used to compute stress distributions. Two boundary conditions were used: a uniform pressure and a sinusoidal, radial pressure distribution with a loading mode number $n=4$, i.e., $p(r_0,\theta)/p_4=\cos(4\theta)$. The calculations were made with a commercially available finite element package *ADINA* (ADINA R & D Inc. 2000).

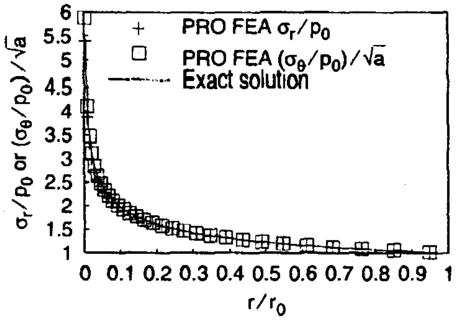

Fig. 3. Stress singularity in cylindrical orthotropy solid, elastic disk subjected to uniform pressure ($a=0.5$)

Results

Uniform Pressure Case: $p(r,\theta)=p_0$

Before considering the general sinusoidal pressure case, the uniform pressure case will be reviewed. The stress function for this case does not depend on θ, i.e., $\phi=\phi_0(r)$. Operating on this form with L of Eq. (7) and solving the resulting differential equation leads to

$$\phi_0(r)=K_{01}+K_{02}r^{1-\sqrt{a}}+K_{03}r^{1+\sqrt{a}}+K_{04}r^2 \qquad (13)$$

The first term, a constant, will generate no stress and can be set equal to zero $K_{01}=0$. The coefficient of the second term must be set equal to zero to ensure finite displacements at the origin $K_{02}=0$. The coefficient of the last term must also be set equal to zero; otherwise, multiple values for the displacements along the ray, $\theta=0=2\pi$, would occur. Thus $K_{04}=0$. The rationale for this last argument is explained well in Timoshenko and Goodier (1970). From the boundary condition $\sigma_r=p_0$ (uniform pressure), the coefficient K_{03} can be determined and the stress components follow

$$\sigma_r/p_0=(r/r_o)^{\sqrt{a}-1}$$

$$\tau_{r\theta}/p_0=0 \qquad (14)$$

$$\sigma_\theta/p_0=\sqrt{a}(r/r_o)^{\sqrt{a}-1}$$

These stress distributions are shown in Fig. 3 for $a=0.5$, a typical value for wood. Both normal stress components exhibit singular

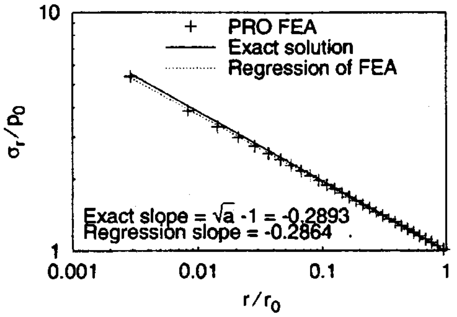

Fig. 4. Linear relationship between logarithm of radial stress and logarithm of radial coordinate

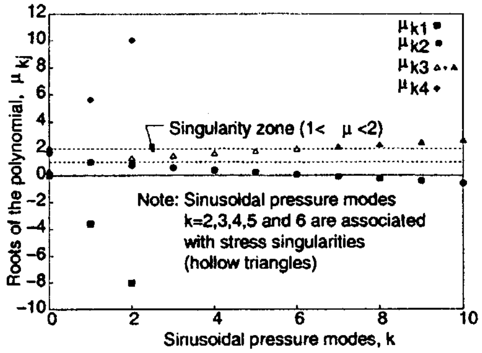

Fig. 5. Roots of characteristic polynomial associated with differential equation for stress function coefficients ($n=0.5$ and $b=10.0$)

behavior near the origin, i.e., the values of stress become infinite as the radial coordinate approaches zero. Also shown in Fig. 3 are the numerical results of the approximating PRO finite element analysis (PRO FEA). Clearly, the numerical results are consistent with the analytical results.

The logarithm of the radial stress is plotted against the logarithm of the radial coordinate in Fig. 4, which shows that the relationship is linear with a slope of $\sqrt{a}-1=-0.2893$, as dictated by the power law of Eq. (14). The results of the FEA are shown in Fig. 4 along with a regression line obtained from the numerical values. The slope of this line has a value of -0.2864. The difference between the two slopes is about 1%. Thus, there is excellent agreement between the analytical and numerical solutions.

Special Case: $p(r,\theta)=p_1\cos(\theta)$ ($n=1$)

If the stress function has the form $\phi=\phi_1(r)\cos(\theta)$, then it can be shown that the general solution for 4, will be

$$\phi_1 = K_{11}r^{1-\chi_{11}} + K_{12}r + K_{13}r\ln(r) + K_{14}r^{1+\chi_{11}} \tag{15}$$

where $\chi_{11}^2=1+a+2b$. The second term, $K_{12}r\cos(\theta)$ will produce no stress, so K,, can be set equal to zero without loss of generality. The coefficients of the first and third terms must be set equal to zero to maintain finite displacements at the origin: hence, $K_{11}=K_{13}=0$. Given a pressure distribution of $\sigma_r=p_1\cos(\theta)$ at the outer boundary of the disk, $r=r_o$, the last coefficient K_{14} can be found and thus the stress distribution in the disk is

$$\sigma_r/p_1 = (r/r_o)^{a+2b}\cos(\theta)$$

$$\sigma_\theta/p_1 = (2+a+2b)(r/r_o)^{a+2b}\cos(\theta) \tag{16}$$

$$\tau_{r\theta}/p_1 = (r/r_o)^{a+2b}\sin(\theta)$$

It is clear that if $\sigma_r=p_1\cos(\theta)$ at the boundary, then a shear distribution $t_{r\theta}=p_1\sin(\theta)$ must also be applied at the boundary to keep the disk in equilibrium. Since we are considering only those cases where no shear stress components occur on the outer boundary of the disk, the term $p_1\cos(\theta)$ must be dropped from the general pressure expression of Eq. (4). In any event, no stress singularities are associated with this pressure mode as the exponent of the radial coordinate, $a+2b$, will never be negative.

General Case: $p(r,\theta)=p_n\cos(n\theta)$ ($n=2,3,\ldots$)

Given a sinusoidal pressure distribution of the form $p=p_n\cos(n\theta)$ for $n>1$, the stress distributions within the solid wood disk are found to be

$$\sigma_r/p_n = \left\{f_1 - \frac{n}{n^2-1}f_2\right\}\cos(n\theta)$$

$$\sigma_\theta/p_n = -\left\{\frac{n}{n^2-1}f_2 + \frac{n^2}{n^2-1}f_3\right\}\cos(n\theta) \tag{17}$$

$$\tau_{r\theta}/p_n = -\left\{\frac{n^2}{n^2-1}f_2\right\}\sin(n\theta)$$

where

$$f_2 = \left\{\left(\frac{r}{r_o}\right)^{n\chi_{n2}-1} - \left(\frac{r}{r_o}\right)^{n\chi_{n1}-1}\right\}\frac{\chi_{n1}\chi_{n2}}{\Delta\chi}$$

$$f_3 = \left\{\chi_{n2}\left(\frac{r}{r_o}\right)^{n\chi_{n2}-1} - \chi_{n1}\left(\frac{r}{r_o}\right)^{n\chi_{n1}-1}\right\}\frac{\chi_{n1}\chi_{n2}}{\Delta\chi}$$

$$\Delta\chi = \chi_{n1} - \chi_{n2}$$

The mathematical form of the expressions in Eq. (17) results from setting K_{n1} and K_{n2} in Eq. (11) to zero. This eliminates infinite displacements at the center of the solid disk since the roots μ_{n1} and μ_{n2} are negative. The other two coefficients, K_{n3} and K_{n4}, are determined by setting the radial stress at the boundary to the sinusoidal pressure distribution and by setting the shear stress at the boundary to zero. Since the root μ_{n4} is always positive and greater than two, terms associated with this root will lead to no displacements or stresses at the disk's center. It is the root μ_{n3} [see Eq. (12) with $k=n$] that gives rise to interesting results. If this root takes on a value greater than two, it will also lead to no displacements and stresses at the center of the disk. However, if it takes on a value between one and two, then the displacement at the center of the disk will be zero but the stress at the center will be infinite. If the root is exactly two, then a finite stress will occur at the center of the disk. It is the value of the quantity $n\chi_{n2}$ that determines whether the stress at the center of the disk is zero, finite, or infinite. This quantity shows up in the exponents in the expressions for f_1, f_2, and f_3 of Eq. (17).

The four roots, μ_{nj}, are represented graphically in Fig. 5 as a function of the loading mode number $k=n$. When $a=0.5$ and $b=10$, there are five sinusoidal loading modes, $n=2$–6, that have roots in the 1–2 interval and consequently produce stress singularities. Since $\mu_{n3}=1+n\chi_{n2}$, the reason for the singularities in the

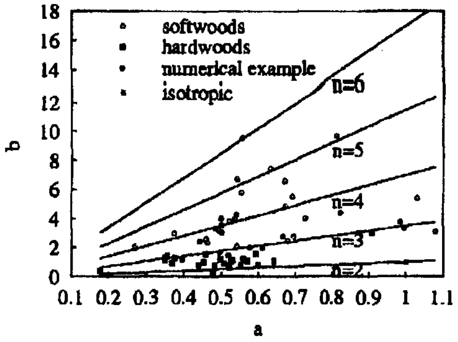

Fig. 6. Dimensionless elastic parameters for wood and singularity separation zones for $p(r,\theta)=p_n\cos(n\theta)$ loadings; $a=E_T/E_R$; and $b=\frac{1}{2}(E_T/G_{RT})-\nu_{TR}$

stress distributions is that $n\chi_{n2}<1$. Substituting $\mu n2=2\,(k=n)$ into Eq. (12) gives $[a(n^2-1)-2b]n^2=0$. It then follows that a stress singularity will occur when $b>a(\frac{1}{2}n^2-1)$.

For a fixed value of *n,* the equation separating the elastic parameter space (a,b) into two zones is

$$b=\left(\tfrac{1}{2}n^2-1\right)a \tag{18}$$

These zones are shown in Fig. 6 for several values of n: 2,3 ... 6. For a given sinusoidal pressure mode number *n,* a stress singularity will occur if the *a, b* coordinates lie above the line associated with the mode number. Those combinations of *a* and *b* values lying below the line will not produce stress singularities. Also shown in Fig. 6 are the a and b coordinates for typical wood species (Bodig and Goodman 1973).

This diagram clearly shows that there is an upper limit on the sinusoidal stress mode number that will produce stress singularities. Given a wood disk with elastic parameters a and b, all modes *n* such that $n>\sqrt{2(1+(b/a))}$ will not generate singularities. If b is large relative to a, however, there may be several lower order modes that will produce singularities. For example, if $b=5$ and $a=0.5$, the modes $n=2$, 3, and 4 will generate singularities, but if a remains the same and b is doubled, two more modes would be added to the list, $n=5$ and 6.

Dimensionless radial and tangential stress components along the ray $\theta=0$ are shown in Fig. 7 for loading mode $n=4$ and for the elastic parameters $a=0.5$ and $b=10.0$. The shear stress distribution along the ray $\theta=\pi/8$ is also shown. The magnitudes of all three components exhibit unbounded increases near $r=0$ as a result of μ_{43} being in the range of 1–2,

The dependence of the stress components on the angular location variable θ is only a function of the multiplicative factors: $\cos(4\theta)$ and $\sin(4\theta)$. Near the center of the disk, the normal stress components change dramatically from tension to compression four times along the circumference of a small circle whose center is located at $r=0$. Moreover, the dilatation strain energy density, the sum of the products of the normal stress and strain components from Eqs. (1) and (17), along the circumference of this small circle would be proportional to $\frac{1}{2}(1+\cos(8\theta))$ and thus would take on eight maximums at $\theta=m\pi/4$ $(m=0,1,\ldots 7)$. This strain energy density would also be zero when $\theta=(2m+1)\pi/8$. However, at these locations the shear strain energy density would be a maximum. Clearly then, zones of maximum dilatation energy densities interleave zones of maximum shear energy densities in the disk subjected to sinusoidal loading mode $n=4$ and the magnitudes of these maximums increase for circles with decreasing radii.

To illustrate the difference between the exact results and those obtained by numerical methods, a few finite element calculations were made. Three elastic parameter cases were considered in conjunction with a loading mode $n=4$. The three elastic parameter combinations are indicated by solid circles in Fig. 6 (labeled: numerical example). The ratio of the Young's moduli was held constant, $a=0.5$, but *b*, the parameter associated with the shear modulus, was chosen to be 3.0, 3.5, and 4.0. The three dimensionless stress components, analytical, and finite element results, for the three cases are shown in each of the parts of Fig. 8. The analytic results indicate that no stress will occur at the center of the disk when $b=3.0$. A state of finite stress will occur at the center when $b=3.5$ and the stress components will "blow up" at the center when $b=4.0$. This reveals the remarkable bifurcation phenomena associated with the values of the elastic parameters of a CYO material.

The finite element results also indicate stress amplification near the disk center for the $b=4.0$ case and show stress decay for the $b=3.0$ case. However, the FE results do not approximate the analytic results very well, particularly near the center of the disk. In the $b=3.5$ case, the FE results are even worse as they indicate a stress decay rather than converging to a finite value at $r=0$. It was not the purpose of this study to construct a precise finite element model to accurately duplicate the analytical results. We were only interested in the degree to which a standard FE analysis would capture the bifurcation phenomena.

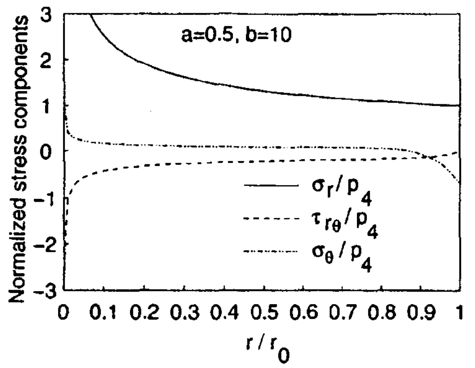

Fig. 7. Stress singularities in all stress components $[\sigma_r(r,0),\sigma_\theta(r,0)$, and $t_{r\theta}(r,\pi/8)]$ for sinusoidal pressure mode $n=4$ with $a=0.5$ and $b=10.0$

Discussion

The dimensionless elastic parameter space, as shown in Fig. 6, is a new way to consider the behavior of orthotropic materials. The existence of stress singularities at the center of the CYO disk for various sinusoidal loading modes and for particular combinations of elastic constants seems bizarre. Obviously, infinite stress never occurs in nature. Thus, the stress singularities are basically mathematical artifacts. They are exhibited by the continuum model that is being used to characterize the behavior of an actual wood disk, an object composed of a biological, porous material consisting of very small hollow cells—fibers—all bound together. It is noted also that the annual rings of trees are not perfect circles composed of uniformly constant elastic material; nor is the trunk of a tree absolutely cylindrical since it is tapered in reality.

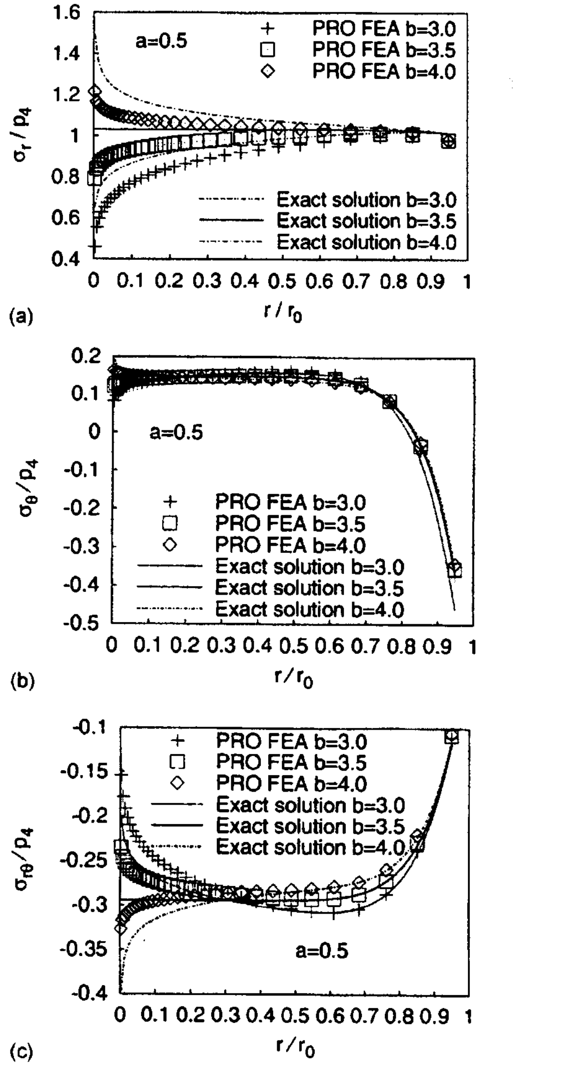

Fig. 8. Comparison between analytical results and finite element approximations ($n=4$) of stress bifurcation at center of cylindrical orthotropy disk (a) Radial stress component $\sigma_r(r,0)$; (b) tangential stress component $\sigma_\theta(r,0)$; and (c) shear stress component $\tau_{r\theta}(r,\pi/8)$

In real trees there is a small region in the center of a tree trunk that is composed of another type of soft material, called pith. The tissue in this region is composed of thin-walled cells with large void spaces. This material is very compliant. It would be more realistic to model this region as a flexible isotropic material or, alternatively, to replace the zone with a hole containing no material. In either case the mathematical model would not produce stress singularities at the center. The material organization, however, would still lead to stress amplifications near the center of the tree. It is the nature of the stress amplification that is of interest here.

The intriguing aspect of our findings is the three distinctly different patterns of stress for different values of dimensionless elastic constants under various loading conditions. In the case of a uniform pressure, one can intuitively imagine how the bifurcation can physically develop. Suppose that the solid disk is cut into several concentric rings. Separate these rings and subject the outer ring to a uniform pressure on its outer circumference. The ring will deform and the inner circumference will squeeze into a smaller circle. Now subject the next smaller ring to another pressure such that its outer displaced circumference is equivalent to the inner circumference of the loaded outer ring. Continue this mental process. Apply sufficient pressure to the outer circumference of any ring so that its displaced shape conforms to the inner circumference of the next largest ring. A sequence of pressure values will be generated by this process. They represent the pressures each ring must be subjected to so that all the rings will fit together and form the solid loaded disk, i.e., there will no gaps between the rings.

If the disk is composed of an isotropic elastic material, $a=1$, then all the pressure values in the list will be the same. The state of stress is uniform in the disk. If, however, the material is stiffer along the circumference, in the tangential direction than along the rays in the radial direction, then the total length of the deformed circumference will be less than that of the isotropic case and the radial displacement will be smaller. Less pressure will be required to compress the next ring, and even less for the next after that. A monotonic decreasing sequence of pressures will be obtained. An infinite sequence of pressures with a limit of zero will result if the number of rings is increased and the rings become thinner and thinner. Thus, for $a>1$ the stress in the center of the disk will converge to zero.

Just the opposite would occur for a set of rings whose stiffness is greater in the radial direction than the tangential. In this case, more pressure has to be applied to each successive ring to squeeze the rings so they tit together in the loaded state. Now the sequence of pressure values will increase. For an infinite number of infinitesimally thin rings, the sequence will have no limit; the pressure values will increase without bound. The center of the disk with $a<1$ will have an infinite stress.

A more complicated situation is encountered when the disk is subjected to a sinusoidal pressure at the outer Circumference. Imagine again that the disk is separated into concentric rings. The outer ring will be subjected to an alternating pattern of tension and compression cycles. A state of shear will develop in those regions where there is a tangential gradient in the pressure distribution. Thus, in addition to a pressure distribution, a shear distribution will have to be applied to the outer circumference of the next ring so that its displaced shape is compatible with the inner circumference of the outer disk.

Suppose now that the shear modulus is large, or conversely that b is small. In this case, little shear deformation will occur. It can be conjectured that this "shear stiffening" might decrease the pressure and shear compensation that must be placed on the outer circumference of the next smaller ring to maintain displacement continuity. The maximum values of the pressure and shear distributions for the following sequence of rings would decrease. If the shear modulus is small (large b), then it appears that the pressure and shear distributions acting on the next smaller rings must be increased to preserve displacement continuity. For the right combination of shear resistance and the ratio of Young's moduli, there is a delicate balance between the displaced shapes of the concentric rings that leads to a finite state of stress at the center of the disk. Without the help of the mathematical solutions, it is difficult to intuitively understand this delicate balance between the shape and volume changes.

The finite element stress distribution calculations of the uniform pressure case (Fig. 3) matched the analytical results very well. This was an axisymmetric case with no shear component. In the case of sinusoidal loading, however, the finite element and analytic results (Fig. 8) were not well matched but, by and large, the bifurcation in stress results relative to the values of the elastic constants did show up. There are several possible explanations for this discrepancy. The mesh may not have been optimized for this problem. The apparent delicate balance between normal strain and shear strain in this problem seems to create difficulties with respect to a traditional FE analysis. The use of rectilinear orthotropic material in a patchwise fashion, such that there is a small but finite mismatch of material properties across the element boundaries, could have led to some errors. Or, the equivalent loads, applied to the outer circumference representing the sinusoidal pressure distribution, may have caused some problems. Resolving the computational discrepancies will be left for future research.

The relevance of sinusoidal pressures may not be immediately obvious, but such loads are a first step in modeling other loading conditions that may be induced by such practical situations as drying of a log. The bifurcation phenomena suggests that center point cracking will result in some log cross sections but possibly not others because of material variability in the same tree.

Conclusions

Stress singularities can occur in solid disks of cylindrically orthotropic elastic material subjected to sinusoidal pressure distributions at the outer boundaries. For a particular combination of two dimensionless elastic property parameters, there are only a finite number of sinusoidal loading modes that produce stress singularities. A finite element analysis, utilizing a rectilinear orthotropic material assumption for the material in each element, exhibited the bifurcation phenomena found in the analytic results but was unable to accurately duplicate the exact results. Whether or not the CYO material assumption is valid for modeling the mechanical behavior of wood is still an open question, but it is one worthy of further inquiry.

Acknowledgment

This research was funded by a grant from the USDA NRI Competitive Grant Program, Grant No. 93-37103-9484.

Notation

The following symbols are used in this paper:

a = E_T/E_R, dimensionless elastic parameter;
b = $\frac{1}{2}(E_T/G_{RT})-\nu\sqrt{a}$, dimensionless elastic parameter;
D_k = differential operators, $k=1\ldots6$;
E_i = modulus of elasticity in direction i;
$\hat{\mathbf{e}}_i$ = unit vector in coordinate direction i;
f_k = substitution variable defined in Eq. (17);
G_{ij} = shear modulus in plane ij;
K_k = constants of integration, $k=1\ldots4$;
L = axis aligned with wood fibers in tree;
L = fourth order differential operator;
P_k = substitution variable defined in Eq. (10);
p = self-equilibrating pressure acting on surface;
R = axis aligned with radial direction;
r = radial axis in cylindrical coordinate system, or radial distance in disk;
T = axis aligned with growth ring tangent;
y = substitution variable defined in Eq. (17);
z = longitudinal axis in cylindrical coordinate system;
γ_{ij} = shear strain in plane ij;
ε_i = small normal strain tensor in coordinate direction i;
θ = tangential axis in cylindrical coordinate system;
μ_j = roots of the characteristic polynomial;
ν = $\sqrt{\nu_{RT}\nu_{TR}}$;
ν_{ij} = Poisson's ratio for plane ij;
σ_i = normal stress tensor component in direction i;
τ_{ij} = shear stress component in plane ij;
ϕ = Airy stress function;
$\phi_k,\bar{\phi}_k$ = Fourier coefficients, $k=1\ldots\infty$; and
$\chi_{k1,k2}$ = substitution variable defined in Eq. (12).

References

ADINA R & D, Inc. (2000). *ADINA users manual–Version 7.5,* Watertown, Mass.

Antmann, S. S., and Negron-Marréro, P. V. (1987). "The remarkable nature of radially symmetric equilibrium states of aeolotropic nonlinearly elastic bodies." J. *Elast.,* 18, 131–164.

Archer, R. R. (1987). *Growth stresses and strains in trees,* Springer, New York.

Bodig, J., and Goodman, J. R. (1973). "Prediction of elastic parameters for wood." *Wood Sci.,* 5(4), 249–264.

Bodig, J., and Jayne, B. A. (1982). Mechanics *of wood and wood composites,* Van Nostrand Reinhold, New York.

Forest Products Laboratory. (1999). *Wood handbook: Wood as an engineering material,* No. FPL-GTR-113, U.S. Dept. of Agricultural Forest Services Forest Products Laboratory, Madison, Wis.

Hearmon, R. F. S. (1961). *An introduction to applied anisotropic elasticity,* Oxford University Press, London.

Hermanson, J. (1992). "A finite element analysis of the influence of curvilinear orthotropy on the state of stress in a plate with a hole." MS thesis, Univ. of Washington, Seattle.

Horgan, C., and Baxter, S. C. (1996). "Effects of curvilinear anisotropy on radially symmetric stresses in anisotropic linearly elastic solids." J. *Elast.,* 42(1), 31–48.

Johnson, J. A. (1975). "Hygro-thermoelastic stresses in the transverse section of wood treated as cylindrically orthotropic material." PhD thesis, Univ. of Washington, Seattle.

Kollman, F. F. P., and Côté, W. A. (1964). *Principles of wood science and technology,* Springer, Berlin.

Lekhnitskii, S. G. (1963). *Theory of elasticity of an anisotropic elastic body,* Holden-Day, San Francisco.

Roisum, D. R. (1994). *The mechanics of winding,* TAPPI, Atlanta.

Timoshenko, S. P., and Goodier, J. N. (1970). *Theory of elasticity,* McGraw-Hill, New York.

Ting, T. C. T. (1997). "The remarkable nature of cylindrically anisotropic elastic materials exemplified by an anti-plane deformation." *J. Elast.,* 49(3), 269–284.

Ting, T. C. T. (1999a). "New solutions to pressuring, shearing, torsion and extension of a cylindrically anisotropic elastic circular tube or bar." *Proc. R. Soc. London, Ser. A,* 455, 3527–3542.

Ting, T. C. T. (1999b). "The remarkable nature of cylindrically orthotropic elastic materials under plane strain deformations." *Q. J. Mech. Appl. Math.,* 52(3), 387–404.

Ting, T. C. T. (1999c). "The remarkable nature of radially symmetric deformation of spherically uniform linear anisotropic elastic solids." *J. Elast.,* 53, 47–64.